ACS APPLIED MATERIALS & INTERFACES

Research Article

www.acsami.org

Ion-Directed Assembly of Gold Nanorods: A Strategy for Mercury Detection

Tiziana Placido,[†,∥,‡] Gemma Aragay,[§,‡] Josefina Pons,[⊥] Roberto Comparelli,[†] M. Lucia Curri,*[,†] and Arben Merkoçi*[,§,¶]

[†]CNR-IPCF Istituto per i Processi Chimici e Fisici, Sez. Bari, c/o Dip. Chimica Via Orabona 4, 70126, Bari, Italy

[∥]Università degli Studi di Bari−Dip. Chimica, Via Orabona 4, 70126, Bari, Italy

[§]Nanobioelectronics and Biosensors Group, Institut Català de Nanotecnologia, 08193, Bellaterra, Spain

[⊥]Department of Chemistry, Universitat Autònoma de Barcelona, 08193, Bellaterra, Spain

[¶]ICREA, Barcelona, Spain

Supporting Information

ABSTRACT: Water-soluble gold nanorods (Au NRs) have been functionalized with an *N*-alkylaminopyrazole ligand, 1-[2-(octylamino)ethyl]-3,5-diphenylpyrazole (PyL), that has been demonstrated able to coordinate heavy metal ions. The *N*-alkylaminopyrazole functionalized Au NRs have been characterized by electron microscopy and spectroscopic investigation and tested in optical detection experiments of different ions, namely, Zn^{2+}, Cd^{2+}, Hg^{2+}, Cu^{2+}, Pb^{2+}, and As^{3+}. In particular, the exposure of the functionalized NRs to increasing amounts of Hg^{2+} ions has resulted in a gradual red-shift and broadening of the longitudinal plasmon band, up to 900 nm. Interestingly, a significantly different response has been recorded for the other tested ions. In fact, no significant shift in the longitudinal plasmon band has been observed for any of them, while a nearly linear reduction in the plasmon band intensity versus ion concentration in solution has been detected. The very high sensitivity for Hg^{2+} with respect to other investigated ions, with a limit of detection of 3 ppt, demonstrates that the functionalization of Au NRs with PyL is a very effective method to be implemented in a reliable colorimetric sensing device, able to push further down the detection limit achieved by applying similar strategies to spherical Au NPs.

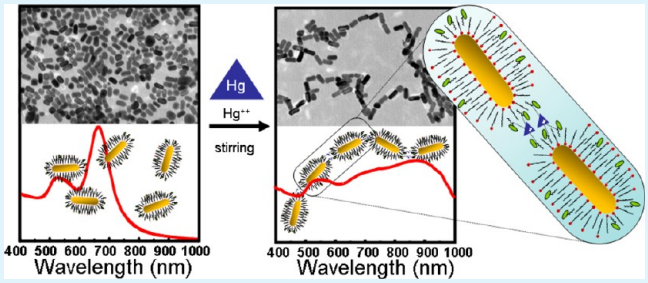

KEYWORDS: *assembly, functionalization, gold nanorods, mercury, sensing*

1. INTRODUCTION

Au nanorods (NRs) have attracted increasing interest thanks to the unique properties arising from their anisotropy. The two distinct plasmon bands, characteristic of such NRs, are due to the oscillation of electrons along the transverse and longitudinal axis, and the position of the longitudinal surface plasmon resonance (SPR) band can be tuned as a function of NR aspect ratio within the visible and near-infrared region.[1,2]

The longitudinal SPR in Au NRs is extremely sensitive, even more than the plasmon absorption detectable in spherical NPs, to any change in dielectric properties of the surrounding environment, including specific solvent and possible presence of adsorbate. A remarkable longitudinal SPR sensitivity has been also reported to interparticle distance between Au NRs. Indeed, new hybridized plasmon modes have been found arising as a function of the arrangements of the NRs, typically turning out in a significant shift and a concomitant broadening of the SPR band, which can be readily observed, even by naked-eye, down to nanomolar concentrations.[3] In addition, such a sensitivity increases as a function of the NR aspect ratio.[4] Therefore, such an assembly process can be observed in situ by following changes in the optical spectrum of the Au NR solution. This unique optical property of Au NRs opens up original applications in biological and chemical sensors. So far, two types of sensors have been mainly developed, based on the specific origin of the change observed in the longitudinal SPR: (i) aggregation based sensors, using the color change due to the near-field electromagnetic coupling induced in NP aggregates, and (ii) refractive index based sensors, relying on the longitudinal SPR peak shift due to the variation in the local refractive index, such as those induced by molecular interactions at the surface of the NPs.[5]

Commonly, Au NRs are produced by means of methods that make them stabilized in aqueous solution by a bilayer of surfactant, typically based on cetyltrimethylammonium bromide (CTAB).[6−8] The peculiar nanoparticle geometry yields local density of CTAB lower at the tips of the rods than along their sides, thus allowing molecules possessing good affinity for

Received: November 27, 2012
Accepted: January 10, 2013
Published: January 10, 2013

Au to easily displace CTAB and bind to the tips of the Au rods. The use of suitable bifunctional molecules has been reported then to induce end-to-end assembly of the NRs.[9,10]

1-D assembly of Au NRs has been widely investigated especially in the biomedical field, owing to their high recognition specificity and selective binding ability on a molecular level.[11−20] A NR based system could be extended to the environmental field, for instance, for heavy metal detection. Mercury is a very toxic element for living organisms, even at low concentration, and its toxicity also depends on the chemical status in which it is found in the environment.[21] Therefore, the development of original methods to detect traces of Hg^{2+} ions in wastewater and in biological systems is extremely relevant for controlling mercury pollution.[22,23] Several sensors have proven to be effective for Hg^{2+} monitoring, including biosensors,[24,25] chemical sensors,[26−29] nanosensors, microcantilever sensors, and piezoelectric sensors.[22]

However, efforts are constantly made to develop simple and cost-effective new sensing strategies able to detect Hg^{2+} ions in a real environment as well as in real-time.[30] Small molecule based sensors that rely on spectroscopic and colorimetric methods of detection have been designed and synthesized.[26] Nevertheless, most of these molecules present limitations due to interferences from other metal ions, thus delaying response to Hg^{2+} ions, and/or show a low water solubility.

In this perspective, nanomaterials offer a great potential for designing highly selective, sensitive, and fast heavy metal and, particularly, Hg^{2+}, detection systems.[31,32] Au NPs have been among the first candidates for colorimetric mercury detection thanks to their unique properties.[5,33−36] In the case of functionalized Au NRs, the change in SPR and the concomitant color change due to Au NR aggregation have been demonstrated as being effective in metal ion sensing in solution.[23]

Biomolecules, such as nucleotides or antibodies, can be used as specific ligands for Au NP functionalization.[32,37,38] Such ligands can specifically complex metal ions and lead to optical changes detectable at concentrations in the ppm level.[39−44] Up to date, the calculated limit of detection (LOD) values reported in literature, using (bio)molecule-functionalized spherical Au NPs, for Hg^{2+} detection, range from 4 ppm to 500 ppt.

An interesting candidate molecule as Au functionalizing agent has been found to be a pyrazole-derived amino ligand (PyL).[45,46] Such a molecule has already been studied for heavy metal detection due to its remarkable ability in heavy metal ion selective coordination, possessing, in particular, a high affinity to Hg^{2+}. PyL capped Au NPs have demonstrated the ability to detect down to 10 ppb of Hg^{2+}.[47]

Here, the goal is to evaluate the detecting ability of Au NRs upon functionalization with this ligand. So far, only few reports have been presented on the use of Au NRs for heavy metal detection.

Au NRs have been used to detect Hg^{2+} in tap water. Chemical reactions of Hg^{2+} with a reducing agent, like $NaBH_4$[48] or ascorbic acid[49] in the presence of Au NRs, have resulted in a local Hg amalgam formation along with a linear assembly of the particles, all accompanied by changes of optical properties of Au NRs.[50] Such a method allowed one to achieve a LOD for Hg^{2+} at the ppt level. However, several other metal ions such as silver, iron, and copper have also been found to induce the change in the SPR extinction of Au NRs, ultimately interfering with the analysis of Hg^{2+}.[51,52]

Ni et al. have prepared methylene blue−Au NR hybrid using electrostatic interactions and studied the effects of various factors like pH, dye composition, and type of metal ions on the resonance coupling between Au NRs and organic dyes.[53] The blue-shift and asymmetric modification of extinction peak caused by the addition of Hg^{2+} in 1−49 μM (0.2−10 ppm) concentration range has been ascribed to the change in the electrical double layer structure and in the local refractive index at the solid−liquid interface around the hybrid nanostructures caused by relatively high concentration of the metal ions. Finally, Wang et al. have reported a selective approach for end-to-end assembly of Au NRs based on the specific recognition between thymine-rich DNA and Hg^{2+} in the concentrations ranging from 1 to 15 μM (0.2−3 ppm) of Hg^{2+}.[54]

In this work, Au NRs, synthesized with specific chemical and physical properties using a suitable modification of a seed-mediated approach,[55−57] have been subsequently functionalized with a pyrazole-derived amino ligand (PyL). The functionalized Au NRs have been characterized by means of UV−vis absorption and FTIR-ATR spectroscopy and transmission electron microscopy (TEM). Finally, Hg^{2+} detection tests have been performed, monitoring by means of UV−vis absorption spectra the addition of Hg^{2+} ions, along with other heavy metal ions, namely, Zn^{2+}, Cd^{2+}, Hg^{2+}, Cu^{2+}, Pb^{2+}, and also As^{3+} ions to the solution of functionalized NRs. The system has demonstrated a remarkable selectivity for Hg^{2+}, pushing the LOD down to 3 ppt. The metal sensing process has been found to be based on detection of a significant change in the spectroscopic features of the functionalized Au NR solution. Namely, a remarkable shift in the maximum of the longitudinal plasmon band has been observed and reasonably related to aggregation phenomena occurring among Au NRs in the presence of Hg^{2+} ions. For the other investigated ions, only a gradual reduction of intensity of the plasmon bands upon increasing amounts of the ions has been detected, without any significant band shift. In the former case, thus, a different sensing mechanism seems to take place, based on a change in the local chemical environment of the Au NRs upon interaction with the different tested ions, i.e., a localized surface plasmon resonance (LSPR) mechanism. Therefore, the reported functionalized nanostructures seem to be promising in Hg sensing and in its chemical discrimination toward other relevant heavy metal ions.

2. EXPERIMENTAL SECTION

2.1. Materials. Hydrogen tetrachloroaurate(III) trihydrate ($HAuCl_4 \cdot 3H_2O$, ≥99.9%), cetyltrimethylammonium bromide (CTAB, ≥96%), silver nitrate ($AgNO_3$, 99.9999%), L-ascorbic acid (99%), and sodium borohydride ($NaBH_4$, ∼99%) were purchased from Aldrich. Cyclohexane (≥99.5%) and acetone (99.8%) were obtained from Fluka. AAS grade standard solutions (Zn^{2+}, Cd^{2+}, Hg^{2+}, Cu^{2+}, Pb^{2+}, and As^{3+}) and HCl (32%) were purchased from Panreac. Diluted stock ion solutions were prepared using deionized water (Millipore milli-Q Gradient A-10 system).

2.2. Synthesis of Ligand and Au NRs. The 1-[2-(octylamino)-ethyl]-3,5-diphenylpyrazole ligand (PyL) was prepared according to a previously reported procedure.[44] PyL ligand, being hydrophobic, has been solubilized in HCl solution (0.1 M) to obtain a 2×10^{-5} M concentration solution (pH = 1).

Water-soluble Au NRs were synthesized using a seed mediated method, adapting a previously reported approach.[55−57] Briefly, the preparation of seeds (<3.5 nm) was performed at room temperature by reduction of Au salt (5 mL of $HAuCl_4 \cdot 3H_2O$, 5×10^{-4} M) with a strong reducing agent (0.6 mL of $NaBH_4$, 0.01 M) in the presence of an appropriate coordinating agent (5 mL of CTAB, 0.2 M).[55] Such a

solution of seeds was kept under stirring for 2 h and then used to grow Au NRs. For this purpose, $HAuCl_4 \cdot 3H_2O$ (0.024 M) was dissolved in 3 mL of CTAB solution (0.08 M), in the presence of 45 μL of cyclohexane and 65 μL of acetone, as well as $AgNO_3$ (Au/Ag = 20), and then reduced by 0.0788 M ascorbic acid (ascorbic acid/Au^{3+} = 2).

As the solution became colorless, a suitable amount of seed solution was added. Then, the solution turned from white to violet−brown, thus suggesting the formation of anisotropic particles. The samples were purified by the excess of free surfactant by centrifugation at 10 000 rpm for 20 min at T = 25 °C. The "as prepared" samples, suitably diluted, were characterized from a spectroscopic and morphological point of view. The purified Au NR solutions showed colloidal stability for several months.

2.3. Functionalization of Au NRs. Purified Au NR solution (0.5 mL, 1.7×10^{-3} M) was dispersed in 2 mL of PyL aqueous solution (2×10^{-5} M). Such a mixture was kept overnight under mild stirring. To purify the solution from the excess of free PyL ligand, the Au NR solution was centrifuged twice at 5000 rpm for 20 min, and the precipitate was redispersed in 5 mL of milli-Q water. Absorption spectra were recorded before and after purification, in order to monitor eventual spectral modification.

2.4. Mercury Detection Test. The functionalized Au NR solution was suitably diluted to obtain 1.7×10^{-4} M for detection tests. Before injecting aliquots of a $Hg(NO_3)_2$ solution (10 ppm), the solution of Au NRs was kept under stirring, undisturbed for 30 min, and monitored by UV−vis absorption measurements to check the stability of the Au NRs in solution under the testing conditions. Then, increasing volumes of a metal ion solution (10 ppm) were repeatedly added to Au NR solution under stirring, and for each addition, after 5 min, the absorption spectrum was recorded. The ligand functionalized Au NRs were used to detect Zn^{2+}, Cd^{2+}, Hg^{2+}, Cu^{2+}, Pb^{2+}, and As^{3+}, respectively, from AAS grade standard solutions, with the same concentrations, ranging within 3−30 ppb. Reported data are presented as mean values with a standard deviation obtained from the analysis of five replicates.

2.5. UV−Visible Spectroscopy. The samples of Au NR solution and detection tests of heavy metal ions were investigated by UV−vis absorption spectroscopy by a SpectraMax M2e spectrophotometer in the 400−1000 nm range. The NR samples were diluted with Millipore water (1:10) after the synthesis, in order to achieve an absorbance value lower than 1 for the longitudinal SPR band.

2.6. Transmission Electron Microscopy (TEM). TEM analyses were performed by both a Jeol JEM-1400 microscope operating at 100 kV and a Jeol JEM-2011 operating at an accelerating voltage of 200 kV. The specimens were prepared by depositing drops of aqueous NP dispersions onto a carbon-coated copper grid and then allowing the aqueous solvent to evaporate. For statistical analysis of Au NR size, shape, and aspect ratio, at least 200 objects were counted for each sample.

2.7. Negative-Staining Transmission Electron Microscopy. Negative-staining technique was applied to investigate the arrangement of surfactants onto the surface of the Au NRs. A small drop of the sample was deposited on the carbon coated grid and allowed to dry. After that, the grid was covered with a small drop of stain solution (2% uranyl acetate). After a few seconds, the drop was blotted dry and the sample was ready for inspection.

2.8. Infrared Spectroscopy. Mid-infrared spectra were acquired with a Varian 670-IR spectrometer equipped with a DTGS (deuterated tryglicine sulfate) detector. The spectral resolution used for all experiments was 4 cm^{-1}. For attenuated total reflection (ATR) measurements, the internal reflection element (IRE) used was a one bounce 2 mm diameter diamond microprism. Cast films were prepared directly onto the internal reflection element, by depositing the solution or suspension of interest (3−5 μL) on the upper face of the diamond crystal and allowing solvent to evaporate. Infrared spectra were recorded in the range of 4000−600 cm^{-1}. Prior to IR measurements, the NRs were further purified upon repeated cycles of dissolution in water and centrifugation to wash out surfactant residuals and free additives.

3. RESULTS AND DISCUSSION

3.1. Functionalization of Au NRs with PyL Ligand. The Au NRs prepared by seed mediated synthesis show the two typical plasmon bands, transverse at 520 nm and longitudinal at 655 nm (Figure 1a). The intensity of the longitudinal plasmon band is higher than that of the transverse one, thus indicating, as the TEM image confirms (Figure 1b), that the particle population is mainly composed of Au NRs, namely, with 2.6 ± 0.4 aspect ratio.

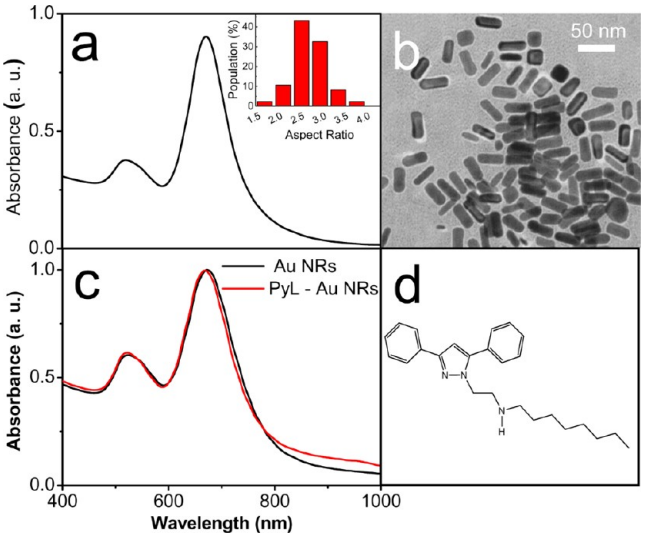

Figure 1. UV−vis absorption spectrum of the Au NRs prepared by seed mediated synthesis (a). Inset: statistic distribution of aspect ratio in the NR sample and TEM micrograph of same NR sample (b). UV−vis normalized absorption spectra of the Au NRs: "as prepared" (black line) and after incubation with PyL (red line), respectively (c), and molecular structure of 1-[2-(octylamino)ethyl]-3,5-diphenylpyrazole (d).

The "as prepared" Au NRs have been incubated overnight in an aqueous ligand solution (2×10^{-5} M). The Au NRs resulting from the incubation process and the subsequent purification step have been investigated by UV−vis absorption spectroscopy, revealing no significant changes in shape and intensity of both plasmon bands, thus allowing the exclusion of relevant particle aggregation (Figure 1c).

The surface of Au NRs has been investigated by comparing FTIR spectra of Au NR samples before and after treatment with ligand (Figure 2 and Table 1). In Figure 2, the FTIR spectra of CTAB (3A), PyL (3B), CTAB-Au NRs (3C), and PyL functionalized Au NRs (3D), in the range of 3600−600 cm^{-1}, are reported. In Figure 2a−d, the corresponding close-up in the region of 1800−600 cm^{-1} is displayed.

The spectra of CTAB and CTAB-Au NRs (Figure 2A-a,C-c) show the typical C−H asymmetric and symmetric stretching vibration at 2918 and 2848 cm^{-1}, respectively. In addition, the bands at 1485 and 1473 cm^{-1} could be ascribed at the bending vibration of N^+-CH_3.[58] Finally, quaternary ammonium mode is observed at 962 and 910 cm^{-1}. The spectrum of PyL (Figure 2B-b) is characterized by the typical bands corresponding to 1605 cm^{-1} $\nu(C{=}C)_{ph}$, 1583 cm^{-1} $[\nu(C{=}C), \nu(C{=}N)]_{pz}$, and 1463 cm^{-1} $[\delta(C{=}C), \delta(C{=}N)]_{ar}$ assigned to the phenyl and pyrazole ring.

In the spectrum of the PyL functionalized Au NR sample (Figure 2D-d), IR signals corresponding to stretching of phenyl

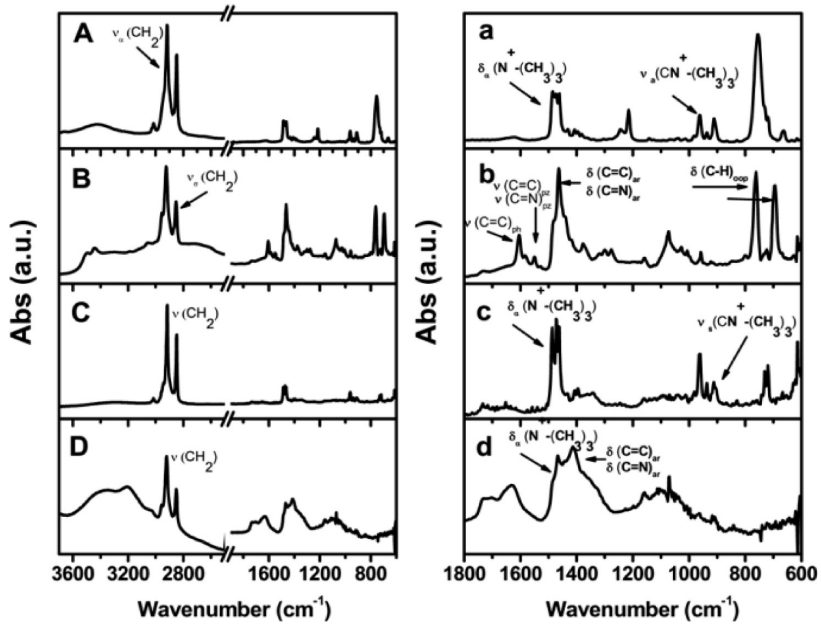

Figure 2. FTIR-ATR spectra of (A) pure CTAB, (B) pure PyL cast from HCl (0.1 M) solution, (C) "as prepared" Au NRs, and (D) Au NRs after treatment with PyL. The right panel reports a magnification of the spectral region ranging between 1800 and 600 cm^{-1} of the corresponding samples.

Table 1. Peak Frequencies (cm^{-1}) and Assignments for CTAB, PyL, "As Prepared" Au NRs, and "PyL Treated" Au NRs

CTAB	PyL	"as prepared" Au NRs	"PyL-treated" Au NRs	assignment
2918	2924	2917	2920	ν_a (CH_2)
2848	2852	2848	2850	ν_s (CH_2)
	1605			ν $(C{=}C)_{ph}$
	1583			ν $(C{=}C)_{pz}$
	1549			ν $(C{=}N)_{pz}$
1485		1486		δ_a $(N^+{-}(CH_3))$
1473		1473	1467	δ_a $(N^+{-}(CH_3))$
	1463		1412	δ $(C{=}C)_{ar}$
				δ $(C{=}N)_{ar}$
1461		1461		δ (CH_2) scissor
962		962		ν_a $(CN^+{-}(CH_3))$
910		910		ν_s $(CN^+{-}(CH_3))$
	762, 694			δ $(C{-}H)_{oop}$

and pyrazole seem not to be present (or anyway below detection limit of the technique). Conversely, signals corresponding to the pyrazole ring, $\delta(C{=}C)_{ar}$, $\delta(C{=}N)_{ar}$, clearly come out, showing a slight shift at 1412 cm^{-1}, possibly due to a weakening of the pyrazole bonds. In addition, the bending of $N^+{-}(CH_3)$ at 1473 cm^{-1} is still detectable, thus suggesting the presence of both CTAB and PyL at Au NR surface.

In conclusion, the IR spectra can confirm the presence of PyL molecule at the Au NR surface, due to the occurrence of specific signals of the ligand in the "PyL treated" Au NRs, which have been incubated with the PyL. No further indication on the coordination mechanism could be definitely inferred at this stage.

Figure 3a shows negatively stained "as prepared" Au NRs, which exhibit a uniformly thick light shell ascribable to organic molecules surrounding the high contrast structure of Au NR. Such a shell, 4 nm thick, can be reasonably attributed to the presence of a CTAB double layer surrounding the NRs.[59] Remarkably, in Figure 3b, the TEM micrograph shows how, after the NR functionalization with PyL, the appearance of the light band surrounding the metal core looks definitely different. In fact, the shell surrounding the darker core, while it seems to retain the same thickness along the side of the rod, it looks much thinner at the tips. Such evidence suggests that a modification of shell would mainly occur at the tips of Au NRs, probably due to a specific positioning of the ligand upon the incubation process.

However, while clear evidence of the successful functionalization is provided by FTIR and TEM analysis, it is less straightforward to define the PyL topology at the Au NR surface. Ligand molecules can be realistically thought not to fully replace the pristine CTAB bilayer, but instead, to occupy hydrophobic domains in the surfactant layer surrounding the NRs, thus resulting only in a slight modification of the pristine structure. Indeed, partitioning of organic molecule into surfactant bilayer coating Au NRs has been reported.[59] Such a feature can be compatible with the higher curvature radius of the tip, which rendering surfactant bilayer less compact, makes PyL molecules likely to preferentially occupy this region, concomitantly breaking this specific portion of the external bilayer structure. However, it cannot be excluded that PyL molecules sit also in the more compact bilayer of surfactant along the long side of the rod.

Such indications would satisfactorily agree with the occurrence of an organic shell thinner at the tip of the functionalized NRs, as observed in negatively stained TEM images. In addition, the more polar moiety of the PyL molecule, that possesses a partial positive charge under the experimental pH conditions, would tend to avoid repulsion with the homologous charge at CTAB polar head, thus possibly intercalating, and/or partially replacing the CTAB molecules in the bilayer. Such an effect would be more marked at the tip of the rods, where ligand molecules present the amino/pyrazole

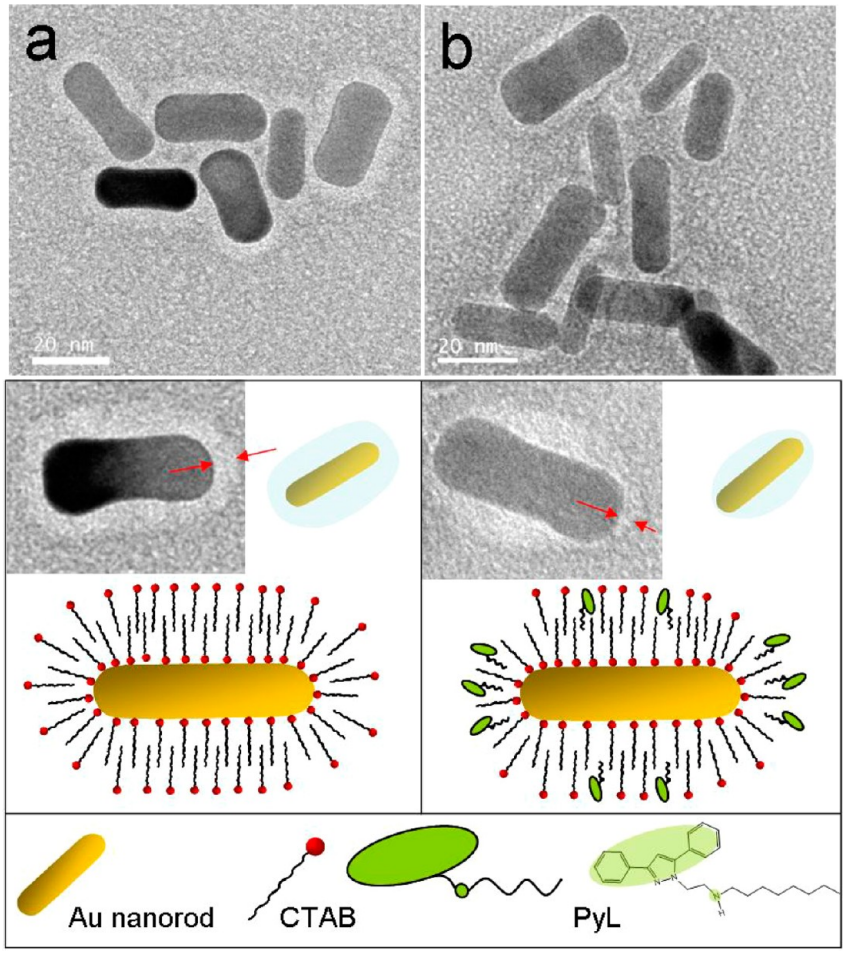

Figure 3. TEM micrographs recorded in negative staining mode of (a) "as prepared" and (b) "PyL treated" Au NRs, respectively. The two samples have both undergone two centrifugation cycles, for 20 min at 5000 rpm. In the lower panel, a sketch of a possible PyL assembly scheme at NR surface.

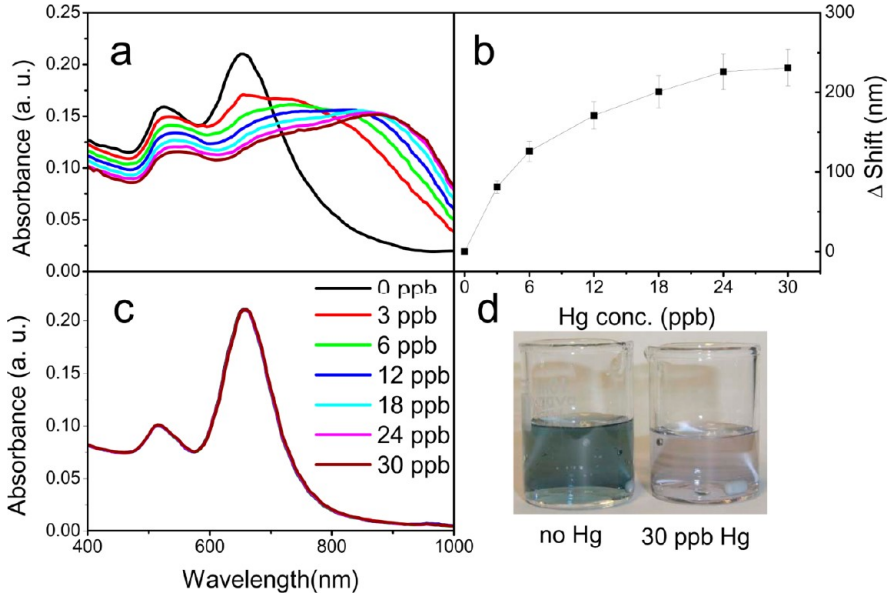

Figure 4. UV–vis absorption spectra of (a) "PyL treated" Au NRs (1.7×10^{-4} M) upon addition of increasing concentration of Hg^{2+} ions (from 0 to 30 ppb), (b) shift of the longitudinal plasmon band at the increasing Hg^{2+} concentration, (c) "as prepared" Au NRs at increasing Hg^{2+} concentration (note an almost overlapping of curves for 0 to 30 ppb), and (d) picture of Au NR solution containing beakers before and after addition of Hg^{2+}. Reported data are presented as mean values with a standard deviation obtained from the analysis of five replicates.

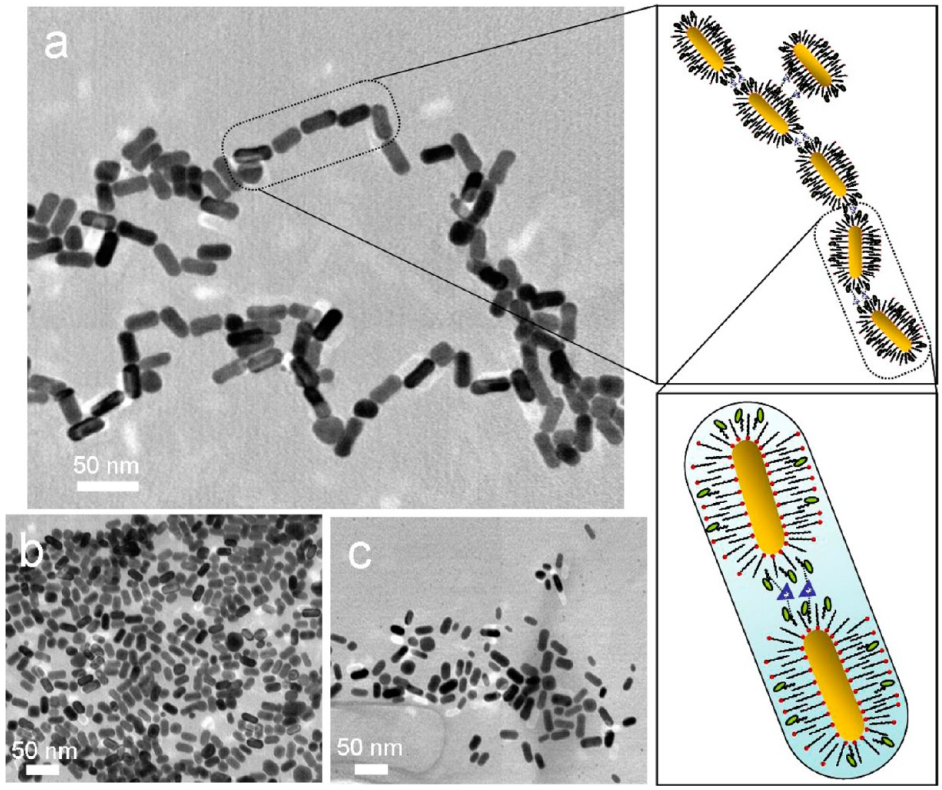

Figure 5. TEM micrographs of PyL functionalized Au NRs before (b) and after (a) addition of 30 ppb of $Hg^{2+}$and as-prepared (c) Au NRs after addition of 30 ppb of Hg^{2+}. On the left: sketch of the possible Hg^{2+} ion detection mechanism.

moiety leaning toward the solution, being thus available for interaction with possible analytes in solution.

3.2. Selective Detection Experiments of Hg^{2+} Ions. Different sets of experiments have been performed in order to evaluate the response of the ligand functionalized NRs to several ion types, namely, Zn^{2+}, Cd^{2+}, Hg^{2+}, Cu^{2+}, Pb^{2+}, and As^{3+} ions. Aliquots of each ion solution (10 ppm) have been repeatedly added to Au NR solution (1.7×10^{-4} M) in a concentration range between 3 and 30 ppb.

3.2.1. Detection of Hg^{2+}. In the case of Hg^{2+} ions, the first addition of 3 ppb of the heavy metal solution has resulted in a decrease of the intensity of the plasmon bands and the concomitant red-shift and broadening of the longitudinal band. The color change of solution upon the addition of Hg^{2+} is visible within a few minutes. By further additions of Hg^{2+} solution, the red-shift of the longitudinal band becomes more and more significant, moving from 655 nm up to 900 nm (relative standard deviation = 10%), while the transverse plasmon band has been observed only to decrease its intensity (see Figure S1, Supporting Information), without changing its position (Figure 4a). Figure 4b shows the shift of the longitudinal plasmon band by increasing the Hg^{2+} concentration. The procedure has been found highly reproducible, thus indicating the functionalized NRs as interesting candidate for practical sensing application. Although response is not linear throughout the explored range, the system is still viable for sensing, i.e., considering a narrower range of linearity, namely, concentration intervals where the response can be considered linear (i.e., 0−6 and 6−30 ppb ranges). In the inset (Figure 4d), the picture of the beakers containing the NR solution clearly shows that the color of the solution noticeably changes before and after Hg^{2+} addition, respectively. The fitting line corresponding to 0−6 ppb range of concentrations shows a higher slope and, thus, a sensitivity higher than that found in the second, higher concentration, range. A linear relationship between absorbance maxima and the concentration of Hg^{2+} over the range of 0−6 ppb has been observed ($R = 0.9731$), and the limit of detection (LOD) for Hg^{2+} at a signal-to-noise ratio of 3 was estimated to be 3 ppt.

A set of reference experiments has been carried out on Au NRs prior to the functionalization step, by the addition of the same amounts of Hg^{2+} ion solution, under the same experimental conditions used for the functionalized Au NRs. The registered absorption spectra do not show any change in the plasmon band position and intensity even upon the addition of 30 ppb of Hg^{2+} (Figure 4c).

In Figure 5, TEM images of the ligand-functionalized Au NRs, before and after addition of Hg^{2+} ions to the solutions, are reported. The micrographs clearly demonstrate that "PyL treated" Au NRs retain their shape and size and, interestingly, upon exposure to Hg^{2+} form end-to-end assemblies, which are not evident before Hg^{2+} addition. Such a behavior could be reasonably accounted for by a specific interaction of the Hg^{2+} ions with the aminopyrazole ligand at NR surface (Figure 5a).

In fact, "as prepared" Au NRs not only appear to be insensitive to the presence of Hg^{2+} ions, as demonstrated by the spectra recorded in the above-described reference experiment, but also do not assemble in superstructures (Figure 5c). The observed 1D, end-to-end NR assembly, shown in Figure 5a is consistent with the red-shift of the longitudinal band detected upon Hg^{2+} addition (Figure 4a). The occurrence of such an assembly phenomenon only in the presence of Hg^{2+} suggests that the heavy metal interaction with NRs involves preferably

dx.doi.org/10.1021/am302870b | ACS Appl. Mater. Interfaces 2013, 5, 1084−1092

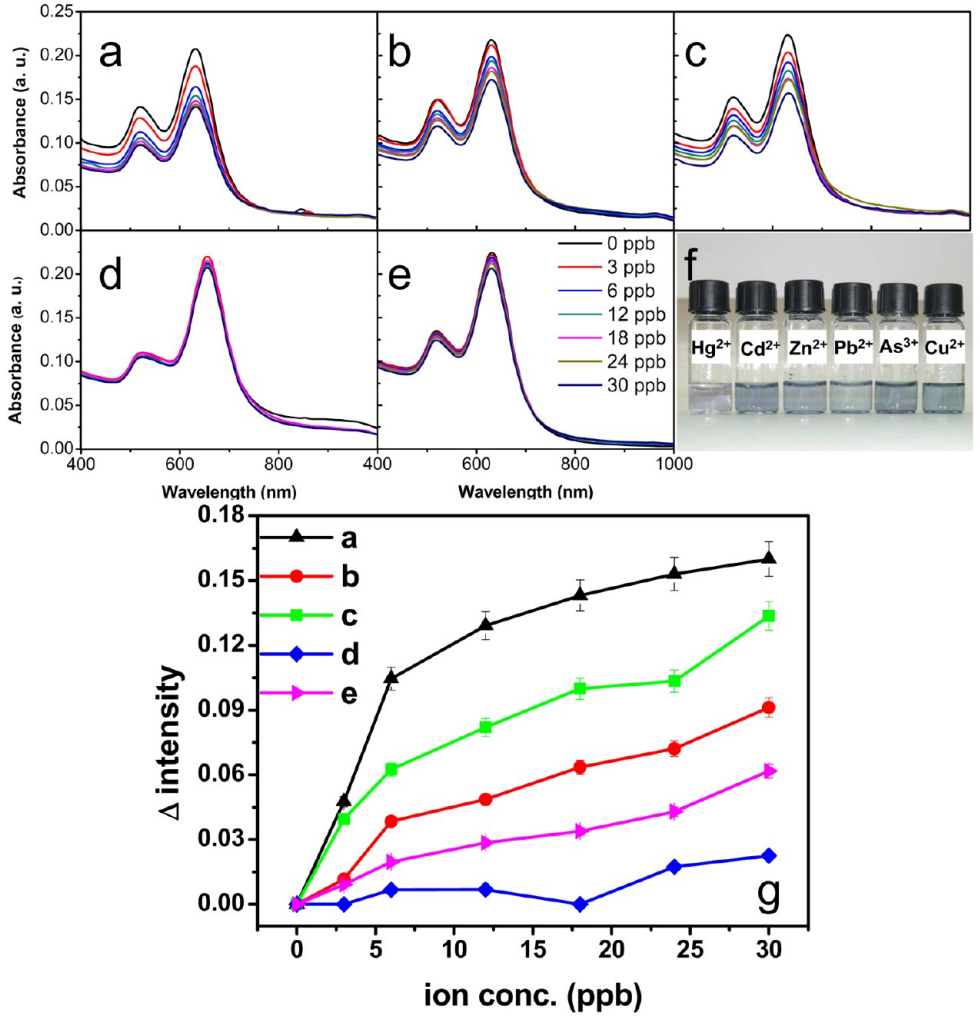

Figure 6. UV−vis absorption spectra of "PyL treated" Au NRs (1.7×10^{-4} M) upon addition of increasing concentration of the different ions: (a) Cd^{2+}, (b) Zn^{2+}, (c) Pb^{2+}, (d) As^{3+}, and (e) Cu^{2+} ions; (f) pictures of relative solutions after ion addition and (g) decrease of absorption intensity recorded at the maximum of the longitudinal plasmon band upon addition of an increasing amount of each cation. Reported data are presented as mean values with a standard deviation obtained from the analysis of five replicates.

their tips, probably due to the specific topology of the ligand in such a region of the NP.

The experimental evidence allows one to safely rule out any responsibility of alternative phenomena, such as formation of an amalgam of Hg with Au. In fact, no blue-shift of longitudinal plasmon band, eventually related to changes in size of Au NRs, due to possible amalgam formation, has been observed (Figure 4c), thus clearly excluding any red-ox process between Hg^{2+} and Au.

3.2.2. Detection of the Other Tested Ions. The spectroscopic response of the PyL functionalized Au NR to the other investigated ions, including several metal ions, appears to significantly differ from that recorded for Hg^{2+} (Figure 6). In fact, while in the presence of Hg^{2+} ions, a broadening and a shift of longitudinal plasmon band has been observed; the presence of other ions in solution has resulted only in a decrease of intensity of such plasmon band, without any detectable shift of its position. The intensity reduction has been found particularly important for Zn^{2+}, Cd^{2+}, and Pb^{2+}, while only a slight decrease has been detected for Cu^{2+} and As^{3+} ions. In all cases, no change in the color of the corresponding solutions after addition of the ion solutions has been observed (Figure 6f).

A linear increase of the intensity absorption reduction, detected at about 650 nm by increasing ion concentration in a range between 3 and 30 ppb, has been observed, with a higher sensitivity in the case of Cd^{2+} and Pb^{2+}, than for Zn^{2+} and Cu^{2+}, and almost no significant response in the case of As^{3+}. Such a decrease in absorption intensity could be due to the ion binding event occurring between pyrazole and/or amine nitrogen in the PyL molecule (possibly in a chelated form) that, inducing also a change in the refractive index at the interface between the Au NRs and solution, may cause a local change in the plasmon bands. (Figure S2, Supporting Information).

The TEM images of PyL-functionalized Au NRs after addition of Pb^{2+}, Cd^{2+}, Zn^{2+}, and As^{3+} ions reported in Figure S3, Supporting Information, clearly highlight the absence of any end-to-end organization of Au NRs upon addition of up to 30 ppb of ions, conversely to what one observed in the case of addition of Hg^{2+}. In addition, in spite of the different extent of the decrease in the absorbance intensity, more pronounced in the case of Cd^{2+} and Zn^{2+}, the optical response cannot be in any case related to any end-to-end aggregation of functionalized Au NRs (Figure S3a,b, respectively, Supporting Information). The longitudinal plasmon band of functionalized Au NRs (Figure 6) does not shift in the case of the ions other than

Hg^{2+}; therefore, the random occurrence of end-to-end connection of Au NRs observed in the TEM micrograph (Figure S3c, Supporting Information) can be thought to occur only upon deposition onto the TEM grid and subsequent solvent evaporation which causes the Au NRs freely dispersed in solution to collapse, forming nearly monolayer quasi-2D structures, reflecting also the spatial anisotropy of the particles.

Conversely, upon addition of Hg^{2+}, the process of Au NR self-organization takes place already in solution as clearly confirmed by the absorption spectra and is clearly not due to solvent evaporation upon sample drying onto the TEM grid.

Although the ability of aminopyrazole functionalized Au NPs has been already reported,[47] the results obtained for the postsynthetic PyL treatment of Au NRs bring new elements to the usage of this sensing molecule in combination with anisotropic NPs. Here, the response to the optical detection mechanism of Zn^{2+}, Cd^{2+}, Cu^{2+}, Pb^{2+}, and As^{3+} ions, using PyL functionalized Au NRs, has been demonstrated to be very different from that one recorded for Hg^{2+}. Both spectroscopic and TEM evidence do not support, in this case, the hypothesis of an ion-triggered assembly or aggregation of Au NRs as it happens during the Hg^{2+} ions detection.

A different sensing mechanism could, then, clearly take place in the case of Hg^{2+} ions. Hg^{2+} ions induce, beside a decrease in absorption intensity of transverse plasmon peak (Figure S1, Supporting Information), a marked shift of the longitudinal band, thus resulting in a remarkable sensitivity (25 nm/ppb), which can be, in addition, also promptly detected due to a color change in solution.

A higher complexation constant for Hg^{2+} than for the other metal ions can reasonably support the peculiar behavior for this element.[60] This consideration would ultimately provide for the Hg^{2+} detection a combination of two mechanisms, namely, a LSPR modification, common also to the other ions, and a specific metal ion induced assembly, responsible for the overall modification in the plasmon absorption band position.

The topology of the ligand at the surface of Au NR plays a clear role in accounting for the high sensing ability of the PyL functionalized NRs. The hypothesis formulated above would suggest a location of PyL molecules mainly at the tip of a rod, leaning toward the solution containing ions, thus resulting more apt to bind, hence to detect, Hg^{2+} ions.

4. CONCLUSIONS

The postsynthesis functionalization of Au NRs with PyL, a pyrazole derived amino ligand, has been presented. The functionalized NRs have been characterized and tested for Hg detection in aqueous solution, along with a series of other ions.

Remarkably, the system has demonstrated a very high sensitivity to Hg^{2+} ions in comparison to the previous Au NP based system.[47] In particular, such a result is related to the ability of Au NR to offer two distinct sensing transduction mechanisms: a general one, common to all the investigated ions, based on the decrease of the surface plasmon band, and a specific one, characteristic for Hg^{2+}, based on the shift of the longitudinal plasmon band. The latter can be explained in terms of a higher complexation constant for such an ion than for the other investigated metal ions. Given the specific longitudinal plasmon band shift specifically related to the end-to-end assembly mechanism, the Au NR can even be considered to be more selective toward Hg^{2+} detection in comparison to Au NP based assays.

The proposed functional material represents a low cost and user-friendly alternative for sensing as the strong red-shift of longitudinal plasmon band can be easily detected and reliably monitored, even at the naked eye, thus offering a prompt transduction system. The obtained results suggest that detection limit could be further pushed down. Although the calculated LOD value for Hg^{2+} at ppt level is comparable with that reached in the extremely sensitive detections performed using the amalgam approach or even by means of fluorescence spectroscopy, in the proposed system, the high sensitivity has been achieved without any chemical reaction or any specific excitation source to activate fluorescence, also being evident at the naked eye. In addition, the simple and general functionalization strategy could be effectively extended to a variety of other amino pyrazole derivatives, in order to screen the sensitivity and selectivity of the molecules to the specific ion. Finally, the role of the Au NR geometry, i.e., length and aspect ratio, could be further and effectively studied in order to fully exploit the potential of this original system and to tailor the response to heavy metal ions.

■ ASSOCIATED CONTENT

Supporting Information

Additional information on detection experiments and on a possible sensing mechanism. This material is available free of charge via the Internet at http://pubs.acs.org.

■ AUTHOR INFORMATION

Corresponding Author

*E-mail: arben.merkoci.icn@uab.es (A.M.); lucia.curri@ba.ipcf.cnr.it (M.L.C.).

Author Contributions

‡These authors contributed equally to this work.

Notes

The authors declare no competing financial interest.

■ ACKNOWLEDGMENTS

The financial support of the Spanish Ministry of Science and Innovation through project PIB2010JP-00278 is acknowledged. G.A. thanks the Generalitat de Catalunya for the predoctoral fellowship (FI 2009). The work has been also partially supported by PRIN 2008 funding programme and by the Sens&Micro LAB Project (2007-2013) funded by Apulia Region (Italy).

■ REFERENCES

(1) Link, S.; Mohamed, M. B.; El-Sayed, M. A. *J. Phys. Chem. B* **1999**, *103*, 3073−3077.
(2) Pérez-Juste, J.; Pastoriza-Santos, I.; Liz-Marzán, L. M.; Mulvaney, P. *Coord. Chem. Rev.* **2005**, *249*, 1870−1901.
(3) Su, K. H.; Wei, Q. H.; Zhang, X.; Mock, J. J.; Smith, D. R.; Schultz, S. *Nano Lett.* **2003**, *3*, 1087−1090.
(4) Jain, P. K.; Eustis, S.; El-Sayed, M. A. *J. Phys. Chem. B* **2006**, *110*, 18243−18253.
(5) Sepúlveda, B.; Angelomé, P. C.; Lechuga, L. M.; Liz-Marzán, L. M. *Nano Today* **2009**, *4*, 244−251.
(6) Liu, M. Z.; Guyot-Sionnest, P. *J. Phys. Chem. B* **2005**, *109*, 22192−22200.
(7) Johnson, C. J.; Dujardin, E.; Davis, S. A.; Murphy, C. J.; Mann, S. *J. Mater. Chem.* **2002**, *12*, 1765−1770.
(8) Nikoobakht, B.; El-Sayed, M. A. *Langmuir* **2001**, *17*, 6368−6374.
(9) Wang, Y.; DePrince, A. E.; K. Gray, S.; Lin, X.-M.; Pelton, M. *J. Phys. Chem. Lett.* **2010**, *1*, 2692−2698.

(10) Nie, Z.; Fava, D.; Kumacheva, E.; Zou, S.; Walker, G. C.; Rubinstein, M. *Nat. Mater.* **2007**, *6*, 609−614.
(11) Sudeep, P. K.; Joseph, S. T. S.; Thomas, K. G. *J. Am. Chem. Soc.* **2005**, *127*, 6516−6517.
(12) Thomas, K. G.; Barazzouk, S.; Ipe, B. I.; Joseph, S. T. S.; Kamat, P. V. *J. Phys. Chem. B* **2004**, *108*, 13066−13068.
(13) Varghese, N.; Vivekchand, S. R. C.; Govindaraj, A.; Rao, C. N. R. *Chem. Phys. Lett.* **2008**, *450*, 340−344.
(14) Shibu Joseph, S. T.; Ipe, B. I.; Pramod, P.; Thomas, K. G. *J. Phys. Chem. B* **2005**, *110*, 150−157.
(15) Nakashima, H.; Furukawa, K.; Kashimura, Y.; Torimitsu, K. *Chem. Commun.* **2007**, 1080−1082.
(16) Bifeng, P.; et al. *Nanotechnology* **2005**, *16*, 1776.
(17) Gole, A.; Murphy, C. J. *Langmuir* **2005**, *21*, 10756−10762.
(18) Caswell, K. K.; Wilson, J. N.; Bunz, U. H. F.; Murphy, C. J. *J. Am. Chem. Soc.* **2003**, *125*, 13914−13915.
(19) Chang, J.-Y.; Wu, H.; Chen, H.; Ling, Y.-C.; Tan, W. *Chem. Commun.* **2005**, 1092−1094.
(20) Vigderman, L.; Khanal, B. P.; Zubarev, E. R. *Adv. Mater.* **2012**, *24*, 4811−4841.
(21) Nolan, E. M.; Lippard, S. J. *Chem. Rev.* **2008**, *108*, 3443−3480.
(22) Selid, P.; Xu, H.; Collins, E. M.; Striped Face-Collins, M.; Zhao, J. X. *Sensors* **2009**, *9*, 5446−5459.
(23) Si, S.; Kotal, A.; Mandal, T. K. *J. Phys. Chem. C* **2007**, *111*, 1248−1255.
(24) Ono, A.; Togashi, H. *Angew. Chem., Int. Ed. Engl.* **2004**, *43*, 4300−4302.
(25) Liu, J.; Lu, Y. *Angew. Chem., Int. Ed. Engl.* **2007**, *46*, 7587−7590.
(26) Nolan, E. M.; Lippard, S. J. *J. Am. Chem. Soc.* **2003**, *125*, 14270−14271.
(27) Guo, L.; Zhang, W.; Xie, Z.; Lin, X.; Chen, G. *Sens. Actuators, B* **2006**, *119*, 209−214.
(28) Zhao, Y.; Lin, Z.; He, C.; Wu, H.; Duan, C. *Inorg. Chem.* **2006**, *45*, 10013−10015.
(29) Segura-Carretero, A.; Costa-Fernández, J. M.; Pereiro, R.; Sanz-Medel, A. *Talanta* **1999**, *49*, 907−913.
(30) Maghasi, A. T.; Conklin, S. D.; Shtoyko, T.; Piruska, A.; Richardson, J. N.; Seliskar, C. J.; Heineman, W. R. *Anal. Chem.* **2004**, *76*, 1458−1465.
(31) Aragay, G.; Pons, J.; Merkoçi, A. *Chem. Rev.* **2011**, *111*, 3433−3458.
(32) Ye, B.-C.; Yin, B.-C. *Angew. Chem., Int. Ed. Engl.* **2008**, *47*, 8386−8389.
(33) Marinakos, S. M.; Chen, S.; Chilkoti, A. *Anal. Chem.* **2007**, *79*, 5278−5283.
(34) Chen, C.-D.; Cheng, S.-F.; Chau, L.-K.; Wang, C. R. C. *Biosens. Bioelectron.* **2007**, *22*, 926−932.
(35) Li, D.; Wieckowska, A.; Willner, I. *Angew. Chem., Int. Ed.* **2008**, *47*, 3927−3931.
(36) Wang, L.; Zhang, J.; Wang, X.; Huang, Q.; Pan, D.; Song, S.; Fan, C. *Gold Bull.* **2008**, *41*, 37−41.
(37) Liu, J.; Lu, Y. *J. Am. Chem. Soc.* **2005**, *127*, 12677−12683.
(38) Wang, Z.; Lee, J. H.; Lu, Y. *Adv. Mater.* **2008**, *20*, 3263−3267.
(39) Yoosaf, K.; Ipe, B. I.; Suresh, C. H.; Thomas, K. G. *J. Phys. Chem. C* **2007**, *111*, 12839−12847.
(40) Lin, S.-Y.; Wu, S.-H.; Chen, C.-h. *Angew. Chem., Int. Ed. Engl.* **2006**, *45*, 4948−4951.
(41) Kim, Y.; Johnson, R. C.; Hupp, J. T. *Nano Lett.* **2001**, *1*, 165−167.
(42) Huang, C.-C.; Chang, H.-T. *Chem. Commun.* **2007**, 1215−1217.
(43) Yu, C.-J.; Tseng, W.-L. *Langmuir* **2008**, *24*, 12717−12722.
(44) Darbha, G. K.; Singh, A. K.; Rai, U. S.; Yu, E.; Yu, H.; Chandra Ray, P. *J. Am. Chem. Soc.* **2008**, *130*, 8038−8043.
(45) Aragay, G.; Pons, J.; García-Antón, J.; Solans, X.; Font-Bardia, M.; Ros, J. *J. Organomet. Chem.* **2008**, *693*, 3396−3404.
(46) Aragay, G.; Pons, J.; Branchadell, V.; Garçia-Antòn, J.; Solans, X.; Font-Bardia, M.; Ros, J. *Aust. J. Chem.* **2010**, *63*, 257.
(47) Aragay, G.; Pons, J.; Ros, J.; Merkoçi, A. *Langmuir* **2010**, *26*, 10165−10170.
(48) Rex, M.; Hernandez, F. E.; Campiglia, A. D. *Anal. Chem.* **2006**, *78*, 445−451.
(49) Wang, G.; Chen, Z.; Wang, W.; Yan, B.; Chen, L. *Analyst* **2011**, *136*, 174−178.
(50) Huang, H.; Qu, C.; Liu, X.; Huang, S.; Xu, Z.; Zhu, Y.; Chu, P. K. *Chem. Commun.* **2011**, *47*, 6897−6899.
(51) Huang, C.-C.; Yang, Z.; Chang, H.-T. *Langmuir* **2004**, *20*, 6089−6092.
(52) Huang, Y.-F.; Huang, K.-M.; Chang, H.-T. *J. Colloid Interface Sci.* **2006**, *301*, 145−154.
(53) Ni, W.; Chen, H.; Su, J.; Sun, Z.; Wang, J.; Wu, H. *J. Am. Chem. Soc.* **2010**, *132*, 4806−4814.
(54) Wang, Y.; Li, Y. F.; Wang, J.; Sang, Y.; Huang, C. Z. *Chem. Commun.* **2010**, *46*, 1332−1334.
(55) Nikoobakht, B.; El-Sayed, M. A. *Chem. Mater.* **2003**, *15*, 1957−1962.
(56) Kim, F.; Song, J. H.; Yang, P. *J. Am. Chem. Soc.* **2002**, *124*, 14316−14317.
(57) Placido, T.; Comparelli, R.; Giannici, F.; Cozzoli, P. D.; Capitani, G.; Striccoli, M.; Agostiano, A.; Curri, M. L. *Chem. Mater.* **2009**, *21*, 4192−4202.
(58) Orendorff, C. J.; Alam, T. M.; Sasaki, D. Y.; Bunker, B. C.; Voigt, J. A. *ACS Nano* **2009**, *3*, 971−983.
(59) Alkilany, A. M.; Frey, R. L.; Ferry, J. L.; Murphy, C. J. *Langmuir* **2008**, *24*, 10235−10239.
(60) Complexation constants (log *K*) of PyL with Zn^{2+}, Cd^{2+}, and Hg^{2+} have been calculated (results nonpublished) to be 8.71, 3.32, and 17.15, respectively, using SQUAD software. This confirms the highest affinity of PyL for Hg^{2+} ions.

NOTE ADDED AFTER ASAP PUBLICATION

This paper was published on the Web on January 22, 2013, with errors in the Acknowledgment paragraph. The corrected version was reposted on January 25, 2013.